



Universiteit
Leiden

The Netherlands

Synthetic, physical and computational chemistry of propeller-shaped polycyclic aromatic hydrocarbons

Ham, A. van der

Citation

Ham, A. van der. (2022, February 24). *Synthetic, physical and computational chemistry of propeller-shaped polycyclic aromatic hydrocarbons*. Retrieved from <https://hdl.handle.net/1887/3276776>

Version: Publisher's Version

License: [Licence agreement concerning inclusion of doctoral thesis in the Institutional Repository of the University of Leiden](#)

Downloaded from: <https://hdl.handle.net/1887/3276776>

Note: To cite this publication please use the final published version (if applicable).

Chapter 6

Summary and prospects

Summary

The presence of a cyclic, π -conjugated, *i.e.* aromatic, system in organic molecules has a drastic impact on their physicochemical behavior. On the one hand, aromaticity is responsible for the many useful properties of these molecules, ranging from having vibrant colors, to their use in nano-electronic devices. On the other hand, aromaticity can be a burden, as it can make the synthesis and handling of these molecules a difficult endeavor. The problems with polycyclic aromatic hydrocarbons (PAHs) become larger with the size of the molecule. Due to their planar structure, molecules can approach each other at short distances, resulting in amplification of the van der Waals forces, also known as π - π stacking interactions, acting between them, thus seriously limiting their solubility. To circumvent this problem, several strategies, outlined in **Chapter 1**, have been devised.

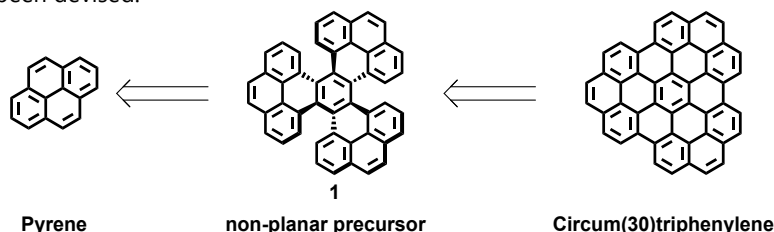
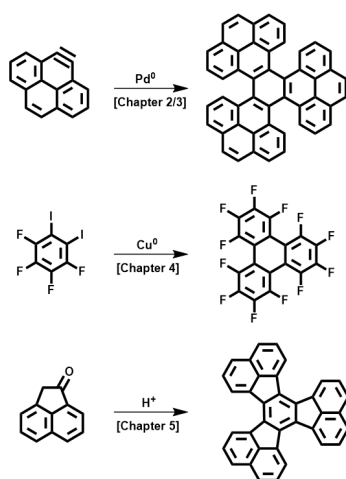


Figure 6.1 Retrosynthetic analysis of the synthesis of circum(30)triphenylene from pyrene *via* a non-planar, propellerene, intermediate.

In the present Thesis, a „non-planar precursor strategy“ was used, with the aim to synthesize the large, planar, PAH circum(30)triphenylene (Fig. 6.1). Synthesis of this molecule was deemed most efficient by ring closure of the non-planar precursor, tripyrenylene **1**. As evidenced throughout this thesis, synthesis of trifold symmetric, propeller-shaped PAHs, *i.e.* propellerenes, can be achieved in different ways (Fig. 6.2). In **Chapter 4**, perfluorotriphenylene, the first ever propellerene, was synthesized by the Ullman coupling of a 1,2-diiodo precursor, whereas in **Chapter 5**, decacyclene was



synthesized by the condensation reaction of acenaphthenone. To obtain tripyrenylene **1**, however, more exotic conditions were needed.

In this case, **1** was obtained *via* the palladium catalyzed trimerization of *in situ* generated alkyne. This route is described in detail in **Chapter 2**, and in brief here.

Figure 6.2 Schematic illustration of different ways in which trimeric PAHs can be obtained, as used in different Chapters in this Thesis. From top to bottom: tripyrenylene **1** (Ch. 2/3), perfluorotriphenylene (Ch. 4), and decacyclene (Ch. 5).

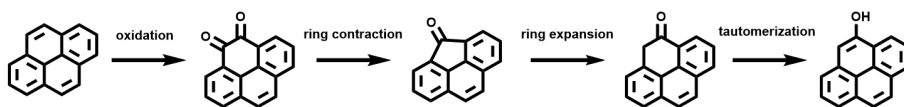


Figure 6.3 Schematic representation of the conversion of pyrene to 4-hydroxypyrene via a ring contraction/ring expansion sequence.

One of the initial hurdles in the synthesis of the non-planar precursor was the inaccessibility of 4-hydroxypyrene. As direct oxidation protocols on pyrene are unable to yield 4-hydroxypyrene, a novel two-step procedure, involving ring contraction and ring expansion, was developed (Fig. 6.3). Bromination and subsequent conversion into an *ortho*-TMS triflate in a three-step-one-pot reaction gave the required intermediate. A palladium catalyzed trimerization then gave the desired propellerene **1** (Fig. 6.4).

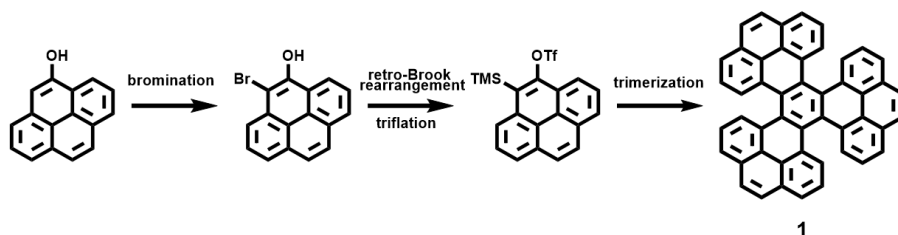


Figure 6.4 Schematic representation of the conversion of 4-hydroxypyrene to propellerene **1** via an *ortho*-TMS triflate.

Although on first inspection tripyrenylene **1** might seem to be flat, steric hindrance actually forces the so-called „wings“ of the molecule to bend out-of-plane, causing the molecule to adopt a non-planar shape. Because of their non-planarity, combined with their trifold symmetry, propellerenes can adopt two possible geometrical configurations. These are the C_2 and D_3 conformation, each of which have their mirror images (Fig. 6.5).

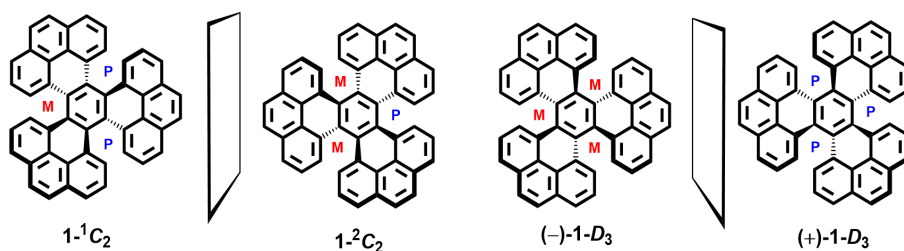


Figure 6.5 The different conformations of propellerene **1**. Structures are given of the C_2 and D_3 conformation, together with their two enantiomers. Chirality of the helical motifs in the molecules are labelled.

The physicochemical properties of propellerenes are dictated by their conformation. A proper understanding of the relationship between the two is thus imperative if they are to be used in a device setting, for example in solar cells. **Chapter 3** details the spectroscopic properties of the different conformations of propellerene **1** as well as the (positional) effect of extension of the π -conjugated system. It shows that the presence of helical motifs is the dictating factor when it comes to the physicochemical properties. Moreover, although extension of the π -conjugated system has a significant impact, the exact position of this extension is of lesser importance.

The conformation propellerenes adopt is, however, no trivial matter, with some propellerenes preferring a C_2 conformation, and others preferring a D_3 conformation. It was Pascal *et al.* who first proposed rules of thumb, aimed at explaining the dichotomy observed between *ortho*-substituted propellerenes and benzoid propellerenes, which prefer a C_2 and D_3 conformation, respectively.¹ These rules are:

- The conformational preference is related to the central ring circumference.
- The conformation of the central ring is not a product of the wings.
- The C_2/D_3 dichotomy is a purely electronic (and not steric) effect.

What is interesting is that they proposed a molecule, colloquially known as „Pascal’s super propellerene“, which defies these rules, by having a circumference greater than 8.6 Å (Fig. 6.6), yet which was computationally predicted to still preferentially adopt a D_3 conformation.

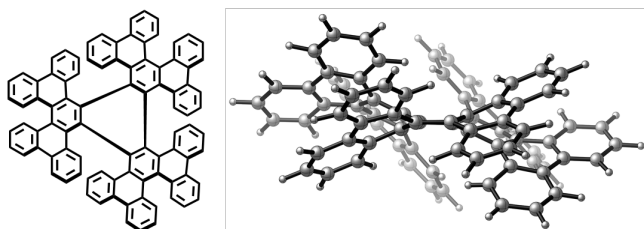


Figure 6.6 Schematic and molecular structure of Pascal’s super propellerene.

Despite its daunting structure, it should be feasible to synthesize this molecule using the methodology outlined in this Thesis (Figure 6.7). The key step is the ring expansion of the known 17*H*-tetrabenzo[*a,c,g,i*]fluoren-17-one with TMS-azidomethane, to yield a phenol, which can be turned into an *ortho*-TMS triflate. Palladium-catalyzed aryne trimerization then yields the super propellerene.

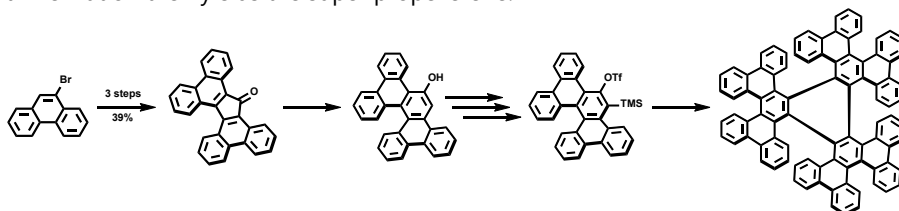


Figure 6.7 Synthetic scheme for the synthesis of Pascal’s super propellerene.

Despite the efforts of Pascal *et al.* and others, no comprehensive model exists to date that can explain the origins of the conformation preference of propellerenes. **Chapter 4** of this Thesis changes this. By computationally dissecting propellerene molecules the preference of their constituent parts was unravelled. It was found that the wings of propellerenes prefer a D_3 conformation, yet their size and rigidity dictate the degree of this preference: the more flexible the wings, the weaker the preference. Combined with a preference of the core and radials bonds for a C_2 conformation, the overall result is *ortho*-substituted propellerenes preferentially adopting a C_2 conformation, and benzoid propellerenes adopting a D_3 conformation. Combined, **Chapters 3** and **4** thus describe the origin of the conformational preference of propellerenes and the effect this preference has on the spectroscopic properties of these molecules, which will ultimately enable the rational design of propellerenes with desired properties.

The strong π - π stacking interactions aromatic molecules can engage in was classified above as a cumbersome property, because of the poor solubility it engenders. **Chapter 5**, however, makes use of this property, showing the formation of a molecularly thin film from the small propellerene decacyclene. The collective action of van der Waals forces acting between the decacyclene molecules allows the formation of a mechanically stable thin film, able to be free-standing over micrometer distances, despite being only 2.5 nm thick. The strength of these thin films could be quantified using state-of-the-art atomic force microscopy (AFM) nano-indentation experiments, showing it to be on par with known 2D membranes. Although no applications of these particular thin films were shown yet, they constitute a first of their kind, showing that covalent cross-linking under harsh conditions is not a prerequisite to form stable membranes from aromatic molecules.

Perspective – PAHs in Astrochemistry

The target molecule of this Thesis was circum(30)triphenylene, a large, planar PAH with D_{3h} symmetry. The electronic nature of the PAH periphery, as well as the symmetry and shape of an aromatic molecule all influence its properties,²⁻⁵ and within the family of planar PAHs, those possessing a D_{3h} symmetry constitute a particularly elusive sub-family. To date, only a handful of homocyclic, unsubstituted PAHs belonging to this sub-family have been synthesized.⁶⁻⁸ They are especially stable with tribenzo(a,g,m)coronene, *e.g.*, having a reported T_1 life time of over 10 seconds.⁸ Similarly, the Raman signal intensity of $C_{96}H_{30}$ was predicted to be greater when the atoms are arranged in a D_{3h} fashion *versus* a D_{6h} one.⁹

The spectroscopic properties of PAHs are of critical importance in the astrochemistry field. The first observations of broad emission bands in the mid-IR range of many emitting stellar regions posed a mystery as to their origins, earning them the title of unidentified infrared emission bands (UIRs).¹⁰⁻¹⁶ Where the first spectra were recorded with ground-based and airborne studies, later studies with the Infrared Space Observatory (ISO; 1995-8) and the Spitzer Space Telescope (SST; 2003-20) much improved the resolution (Fig. 6.8A and B), and showed their ubiquitous presence in the interstellar medium (ISM). The hypothesis that PAHs could be the carriers of these UIRs was first put forward by Allamandola, Tielens and Baker in 1985.¹⁷⁻²⁰ Some 35 years later, the presence of PAHs in the ISM is now well-established. However, the actual composition, *i.e.* the specific molecules, making up these bands, remains uncertain, and only in 2018 was strong evidence provided for the presence of one specific aromatic molecule (benzonitrile) in the ISM.²¹

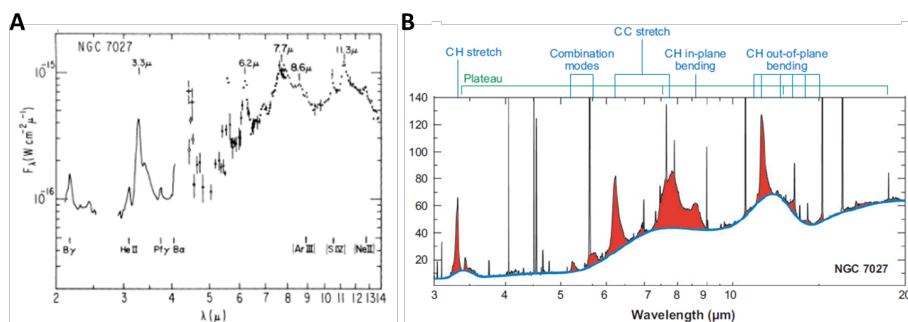


Figure 6.8 The mid-IR spectrum of the photo-dissociation region of NGC 7027 from 1977 (A) and 2002 (B) (Reproduced and adapted from refs. ¹⁶ and ²² respectively).

A further refinement of the PAH hypothesis was made by Alexander Tielens in 2013. From analysis of the energetics involved in the IR emissions, as well as numerous computed reference spectra, a size range of 50 – 150 carbon atoms was established.²²⁻²⁵ The lower limit of C_{50} was additionally supported from the fact that PAHs smaller than this are unstable in the UV field, due to their poor heat capacity.²⁶ This necessity of PAHs to be big in order to serve as emitters of the IR bands is known as the *grand-PAH hypothesis*,²⁷ and much recent research has been divulged in this direction.

The missing link. One question that is central to the grand-PAH hypothesis is: how are they formed? The present axiom is that larger PAHs are formed from smaller ones *via* so-called Hydrogen-Abstraction/Acetylene Addition (HACA) and Hydrogen Abstraction/Vinylacetylene Addition (HAVA) reactions (Fig. 6.9). In this way, C_2H_2 and C_4H_4 fragments can be introduced. In PAH terminology, these represent *K*-region installation and benzene fusion, respectively. It was recently proposed, by Wnuk et al., that the D_{3h} PAHs tribenzo(a,g,m)coronene and circum(30)triphenylene could serve as intermediates in the formation of the stable C_{54} PAH circum(30)coronene in the interstellar medium (ISM).^{28,29} These molecules can be regarded as symmetrical expansions upon a central triphenylene core and their formation is thought off as starting from triphenylene and proceeding *via* a series of consecutive HACA's and HAVA's (Fig. 6.9). Combined with their aforementioned stability and dependence of the vibrational modes on their size, shape and symmetry, the relative scarcity of D_{3h} PAHs makes them ideal candidates for detection in the ISM. A study as to their spectroscopic peculiarities is thus much warranted.

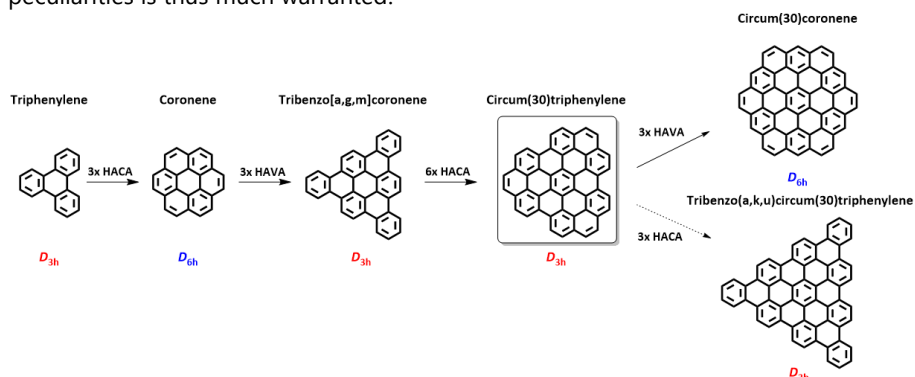


Figure 6.9 Formation of circum(30)coronene as proposed by Zhao *et al.*²⁸ Chemical structures of PAHs are drawn in their Clar structure with the symmetry group they belong to given below. HACA = Hydrogen-Abstraction/Acetylene Addition; HAVA = Hydrogen Abstraction/Vinylacetylene Addition. HACA results in the net introduction of a C_2H_2 unit, HAVA results in the net introduction of a C_4H_4 unit.

With 48 carbon atoms, circum(30)triphenylene lies at the lower limit of the definition of a grand-PAH. Of the D_{3h} PAHs shown in Fig. 6.9, only of circum(30)triphenylene the IR spectrum remains unknown. In light of its potential implications in the hypothesis outlined above, it is desirable to study the IR properties of circum(30)triphenylene both experimentally and computationally.

Apart from constructive PAH transformations, destructive transformations are equally of interest. When excited PAHs are unable to relax *via* IR emission, they undergo photo-fragmentation, mainly *via* the sequential loss of H_2 and C_2H_2 fragments from the molecule. For neutral PAHs larger than $C_{33}H_n$, IR radiative relaxation is predicted to be the dominant mode. For cationic PAHs, formed upon photoionization, relaxation *via* IR emission is dominant regardless of size of the molecule.³⁰ In order to understand the dynamics of PAH(-cation) dissociation, dedicated studies are used that can identify

characteristic fragmentation patterns upon photo-excitation, and the dependence of different fragmentation pathways on, *e.g.*, wavelength and photon intensity. Intuitively, the *K*-regions in circum(30)triphenylene are the most labile part of the molecule,³¹ and one would therefore expect, upon irradiation, sequential loss of C₂H₂ fragments to yield hexabenzocoronene, which then fragments further (Figure 6.10). This hypothesis can be neatly tested, as the fragmentation pathways of the latter are now well documented.³²⁻³⁵

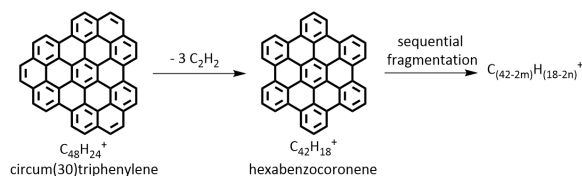


Figure 6.10 Hypothesized fragmentation of circum(30)triphenylene to hexabenzocoronene and beyond. Note that PAHs are drawn as their cationic species, rather than neutral. This aspect will not be considered further here.

Synthesis. The synthesis of circum(30)triphenylene has not been reported before, although its existence was suspected as a high molecular weight pyrolysis product in the combustion of methane.³⁶ A number of substituted^{7,37} and a perchlorinated³⁸ derivative of circum(30)triphenylene have been reported and characterized before, yet the synthetic routes employed there are not amendable for synthesis of the parent structure. Interestingly, circum(30)triphenylene has also been used as a model compound, to computationally study the first-order hydrogenation of graphene.³⁹ It was tried to synthesize circum(30)triphenylene *via* ring closure of tripyrenylene **1** synthesized in **Chapter 2** (Figure 6.11).^{2,40} Several methods to achieve such aromatic ring closures are known, which are collectively known as the Scholl reaction, after Roland Scholl, who reported the synthesis of perylene from naphthalene upon treatment with AlCl₃. Since then, many different conditions have been developed to affect ring closure of aromatic molecules,⁴¹ these include irradiation with UV-light in the presence of iodine, treatment with inorganic oxidizers (*e.g.* AlCl₃, FeCl₃, MoCl₅),⁴² organic oxidizers (*e.g.* DDQ),⁴³ and acids (*e.g.* PIFA).⁴² Of these, only photo-irradiation of **1** as a dilute solution in DCM with a low-pressure mercury vapor lamp was tried, which unfortunately did not yield the desired circum(30)triphenylene. Other reaction conditions remain to be tested.

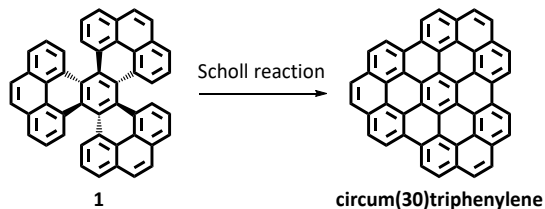


Figure 6.11 Synthesis of circum(30)triphenylene by the Scholl reaction of tripyrenylene **1**.

Infrared. The IR spectra of D_{3h} PAHs can be roughly divided into three regions: i) 700 – 900 cm^{-1} , ii) 1200 – 1600 cm^{-1} and, iii) 3100 – 3300 cm^{-1} (Fig. 6.12A).¹ Absorptions below 700 cm^{-1} originate from vibrations related to ring deformations which will not be discussed here. Region i) contains out-of-plane C – H wagging modes, and can be further refined to solo (900 – 850 cm^{-1}), duo (850 – 800 cm^{-1}) or trio/quarto (800 – 700 cm^{-1}) vibrations.⁴⁴ Region ii) contains C – H wagging modes, and region iii) contains C – H stretching modes. To identify the vibrations associated with difference absorption lines, spectra were computed using DFT computations at the B3LYP/4-31G level of theory, using geometries optimized at the same level. Although seemingly a rather low level of theory, spectra obtained at this level benefit from requiring only a single scaling factor of 0.958 to bring the computed harmonic frequencies into good agreement with experimental fundamentals. It is for this reason its use has become standard in the astro-chemistry field,⁴⁵⁻⁴⁷ and all spectra in the NASA Ames PAH spectral database are computed at this level.⁴⁸ The major absorptions and vibrations in the different regions will now be discussed separately for the different PAHs.

- i) The low wavelength IR region for the fully benzoid PAHs **1** – **3** each has a major absorption corresponding to a collective in-phase, out-of-plane C – H wagging vibration ①, situated at 776, 785 and 794 cm^{-1} , respectively. For circum(30)triphenylene **4**, the frequency of the corresponding vibration is significantly upshifted to 888 cm^{-1} . Compounds **2** and **3** additionally show an absorption corresponding to a collective duo C – H wagging mode at 842 cm^{-1} ②. In triphenylene **1** and **4** such a mode is, obviously, absent, although there are several anti-phase duo wagging modes.
- ii) In the middle wavelength region, the number of absorptions increases greatly with the size of the molecule. Absorptions in this region correspond to different collections of duo C – H rocking ③ and scissoring ④ vibrations. Circum(30)triphenylene **4** shows an additional absorption at 1675 cm^{-1} , corresponding to an anomalous scissoring mode (Fig. S6.1).
- iii) In the high wavelength region two main absorptions are found, each corresponding to different collective anti-phase ⑤ and in-phase ⑥ C – H stretching modes. Interestingly, for the fully benzoid PAHs **1** – **3** the frequency of these absorptions are found to increase only nominally with an increase in size of the molecule. For the larger PAHs **2** – **4** a particular kind of duo “through ring” asymmetric C – H stretching vibration is found ⑦, with circum(30)triphenylene **4**, in turn, uniquely showing a major absorption at 3188 cm^{-1} , corresponding to a mono “through ring” C – H asymmetric stretching vibration ⑧.

¹ In astrochemistry this region is more commonly discussed in terms of 3 – 14 μm (cf. Fig. 6.2).

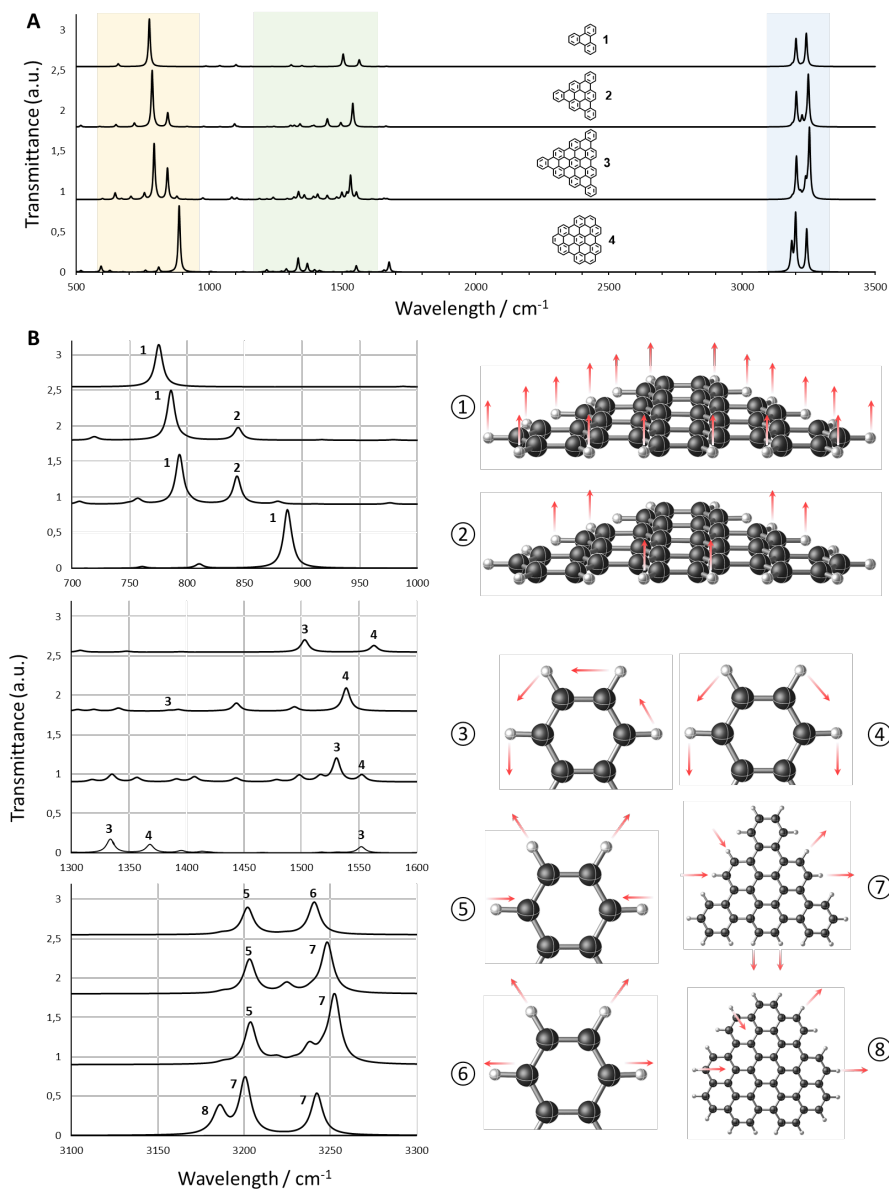


Figure 6.12 (A) Computed IR spectra (at B3LYP/4-31G) of D_{3h} PAHs 1 - 4 (top-to-bottom). (B) Selected regions of the computed IR spectra shown in (A) with the main absorptions in each region labelled. All spectra are to the same scale and arbitrarily offset. Images on the right show the vibrations associated with the corresponding absorption. Vectors not drawn to scale and with arbitrary absolute phase.

From the computational IR study it can be concluded that, although there are broad similarities between the IR spectra of D_{3h} PAHs, the non-fully benzoid circum(30)triphenylene deviates from the general fingerprint, showing distinct features at 888, 1552 and 1675 cm^{-1} . The 888 cm^{-1} vibration in particular (mode ① in Fig. 6.8B) is significantly shifted compared to the corresponding mode in the other PAHs, coinciding with a bright feature in the IRIS nebula (Fig. 6.13). This 11.2 μm band is one of the so-called “unidentified infrared bands” (UIB), and which is currently assumed to be composed of a number of closely packed vibrational modes.⁴⁹

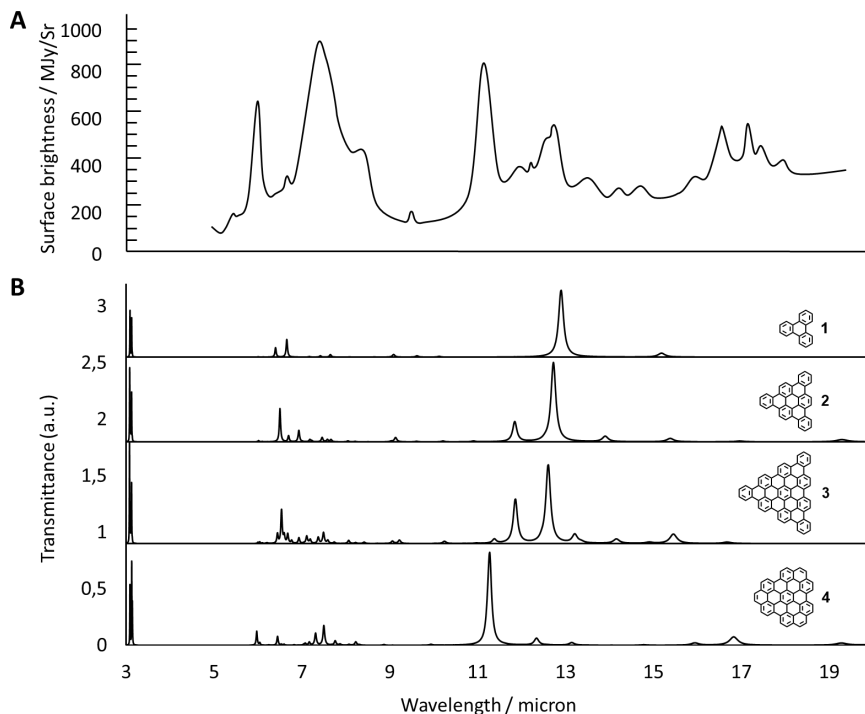


Figure 6.13 Comparison between (A) the experimentally recorded IR spectrum of the dense medium of the northwest photon dominated region of NGC7023; reproduced from ref. ⁵⁰, and (B) computed IR spectra of selected D_{3h} PAHs. Note the coincidence of the 11.2 μm feature in the experimental spectrum, with that computed for circum(30)triphenylene. Note that MJy/Sr in (A) stands for megaJansky per steradian, which is a unit for spectral flux density.

To conclude, with these preliminary results in hand, the next step will be to synthesize circum(30)triphenylene and record its IR spectrum and photo-dissociation spectrum in astronomically similar conditions, in order to confirm or disprove its astrochemical relevance.

References

- (1) Barnett, L.; Ho, D. M.; Baldrige, K. K.; Pascal, R. A. The structure of hexabenzotriphenylene and the problem of overcrowded “D_{3h}” polycyclic aromatic Compounds. *J. Am. Chem. Soc.* **1999**, *121* (4), 727.
- (2) Dias, J. R. Perimeter topology of benzenoid polycyclic hydrocarbons. *J. Chem. Info. Mod.* **2005**, *45* (3), 562.
- (3) Dias, J. R. Phenyl substituted benzenoid hydrocarbons—relationships of the leapfrog algorithm in regard to Clar's sextet rule, strain-free, and perimeter topology concepts. *Polycycl. Arom. Comp.* **2005**, *25* (2), 113.
- (4) Efros, L. S. The aromatic bond and some problems of the structure of aromatic compounds. *Russ. Chem. Rev.* **1960**, *29* (2), 66.
- (5) Reddy, K. V. *Symmetry and Spectroscopy of Molecules*; New Age International, **1998**.
- (6) Zuzak, R.; Castro-Esteban, J.; Brandimarte, P.; Engelund, M.; Cobas, A.; Piątkowski, P.; Kolmer, M.; Pérez, D.; Guitián, E.; Szymonski, M. Building a 22-ring nanographene by combining in-solution and on-surface syntheses. *Chem. Comm.* **2018**, *54* (73), 10256.
- (7) Feng, X.; Wu, J.; Ai, M.; Pisula, W.; Zhi, L.; Rabe, J. P.; Müllen, K. Triangle-Shaped Polycyclic Aromatic Hydrocarbons. *Angew. Chem.* **2007**, *119* (17), 3093.
- (8) Obenland, S.; Schmidt, W. In *Polycyclic Aromatic Hydrocarbons and Astrophysics*; Springer, **1987**.
- (9) Castiglioni, C.; Negri, F.; Rigolio, M.; Zerbi, G. Raman activation in disordered graphites of the A₁ symmetry forbidden k ≠ 0 phonon: the origin of the D line. *J. Chem. Phys.* **2001**, *115* (8), 3769.
- (10) Gillett, F. C.; Forrest, W. J. Spectra of the Becklin-Neugebauer point source and the Kleinmann-Low nebula from 2.8 to 13.5 microns. *The Astrophysical Journal* **1973**, *179*, 483.
- (11) Gillett, F.; Forrest, W.; Merrill, K. 8-13-micron spectra of NGC 7027, BD+ 30 3639, and NGC 6572. *The Astrophysical Journal* **1973**, *183*, 87.
- (12) Gillett, F. C.; Kleinmann, D. E.; Wright, E. L.; Capps, R. W. Observations of M82 and NGC 253 at 8-13 microns. *The Astrophysical Journal* **1975**, *198*, L65.
- (13) Cohen, M.; Anderson, C. M.; Cowley, A.; Coyne, G. V.; Fawley, W.; Gull, T. R.; Harlan, E. A.; Herbig, G. H.; Holden, F.; Hudson, H. S. The Peculiar Object HD 44179 ("The Red Rectangle"). *The Astrophysical Journal* **1975**, *196*, 179.
- (14) Merrill, K. M.; Soifer, B. T.; Russell, R. W. The 2-4 micron spectrum of NGC 7027. *The Astrophysical Journal* **1975**, *200*, L37.
- (15) Grasdalen, G. L.; Joyce, R. R. Additional observations of the unidentified infrared features at 3.28 and 3.4 microns. *The Astrophysical Journal* **1976**, *205*, L11.
- (16) Russell, R. W.; Soifer, B. T.; Willner, S. The 4 to 8 micron spectrum of NGC 7027. *The Astrophysical Journal* **1977**, *217*, L149.
- (17) Allamandola, L. J.; Tielens, A.; Barker, J. Polycyclic aromatic hydrocarbons and the unidentified infrared emission bands-Auto exhaust along the Milky Way. *The Astrophysical Journal* **1985**, *290*, L25.
- (18) Leger, A.; Puget, J. Identification of the 'unidentified' IR emission features of interstellar dust? *Astron. Astrophys.* **1984**, *137*, L5.
- (19) Puget, J. L.; Léger, A. A new component of the interstellar matter: Small grains and large aromatic molecules. *Annu. Rev. Astron. Astr.* **1989**, *27* (1), 161.
- (20) Allamandola, L. J.; Tielens, A.; Barker, J. R. Interstellar polycyclic aromatic hydrocarbons-The infrared emission bands, the excitation/emission mechanism, and the astrophysical implications. *The Astrophysical Journal Supplement Series* **1989**, *71*, 733.
- (21) McGuire, B. A.; Burkhardt, A. M.; Kalenskii, S.; Shingledecker, C. N.; Remijan, A. J.; Herbst, E.; McCarthy, M. C. Detection of the aromatic molecule benzonitrile (c-C₆H₅CN) in the interstellar medium. *Science* **2018**, *359* (6372), 202.
- (22) Tielens, A. The molecular universe. *Rev. Mod. Phys.* **2013**, *85* (3), 1021.

- (23) Peeters, E.; Hony, S.; Van Kerckhoven, C.; Tielens, A.; Allamandola, L. J.; Hudgins, D. M.; Bauschlicher, C. W. The rich 6 to 9 m spectrum of interstellar PAHs. *Astron. Astrophys.* **2002**, *390* (3), 1089.
- (24) Sellgren, K. The near-infrared continuum emission of visual reflection nebulae. *The Astrophysical Journal* **1984**, *277*, 623.
- (25) Ricca, A.; Bauschlicher Jr, C. W.; Boersma, C.; Tielens, A. G. G. M.; Allamandola, L. J. The infrared spectroscopy of compact polycyclic aromatic hydrocarbons containing up to 384 carbons. *The Astrophysical Journal* **2012**, *754* (1), 75.
- (26) Le Page, V.; Snow, T. P.; Bierbaum, V. M. Hydrogenation and charge states of polycyclic aromatic hydrocarbons in diffuse clouds. II. Results. *The Astrophysical Journal* **2003**, *584* (1), 316.
- (27) Andrews, H.; Boersma, C.; Werner, M. W.; Livingston, J.; Allamandola, L. J.; Tielens, A. PAH emission at the bright locations of PDRs: the grandpah hypothesis. *The Astrophysical Journal* **2015**, *807* (1), 99.
- (28) Zhao, L.; Xu, B.; Ablikim, U.; Lu, W.; Ahmed, M.; Evseev, M. M.; Bashkurov, E. K.; Azyazov, V. N.; Howlader, A. H.; Wnuk, S. F. Gas-Phase Synthesis of Triphenylene (C₁₈H₁₂). *Chem. Phys. Chem.* **2019**, *20* (6), 791.
- (29) Stein, S. On the high temperature chemical equilibria of polycyclic aromatic hydrocarbons. *J. Phys. Chem.* **1978**, *82* (5), 566.
- (30) Jochims, H. W.; Ruhl, E.; Baumgartel, H.; Tobita, S.; Leach, S. Size effects on dissociation rates of polycyclic aromatic hydrocarbon cations: Laboratory studies and astrophysical implications. *The Astrophysical Journal* **1994**, *420*, 307.
- (31) Jochims, H. W.; Baumgärtel, H.; Leach, S. Structure-dependent photostability of polycyclic aromatic hydrocarbon cations: Laboratory studies and astrophysical implications. *The Astrophysical Journal* **1999**, *512* (1), 500.
- (32) Zhen, J.; Castellanos, P.; Bouwman, J.; Linnartz, H.; Tielens, A. G. G. M. Infrared spectra of hexa-peri-hexabenzocoronene cations: HBC⁺ and HBC₂⁺. *The Astrophysical Journal* **2017**, *836* (1), 28.
- (33) Palotás, J.; Martens, J.; Berden, G.; Oomens, J. Laboratory IR spectroscopy of protonated hexa-peri-hexabenzocoronene and dicoronylene. *J. Mol. Spectrosc.* **2021**, *378*, 111474.
- (34) Zhen, J.; Paardekooper, D. M.; Candian, A.; Linnartz, H.; Tielens, A. Quadrupole ion trap/time-of-flight photo-fragmentation spectrometry of the hexa-peri-hexabenzocoronene (HBC) cation. *Chem. Phys. Lett.* **2014**, *592*, 211.
- (35) Zhen, J.; Castellanos, P.; Linnartz, H.; Tielens, A. G. G. M. Photo-fragmentation behavior of methyl- and methoxy-substituted derivatives of hexa-peri-hexabenzocoronene (HBC) cations. *Mol. Astrophys.* **2016**, *5*, 1.
- (36) Siegmann, K.; Sattler, K. Formation mechanism for polycyclic aromatic hydrocarbons in methane flames. *J. Chem. Phys.* **2000**, *112* (2), 698.
- (37) Kastler, M.; Schmidt, J.; Pisula, W.; Sebastiani, D.; Müllen, K. From armchair to zigzag peripheries in nanographenes. *J. Am. Chem. Soc.* **2006**, *128* (29), 9526.
- (38) Tan, Y.-Z.; Yang, B.; Parvez, K.; Narita, A.; Osella, S.; Beljonne, D.; Feng, X.; Müllen, K. Atomically precise edge chlorination of nanographenes and its application in graphene nanoribbons. *Nat. Comm.* **2013**, *4*, 2646.
- (39) Boukhvalov, D. W.; Feng, X.; Müllen, K. First-principles modeling of the polycyclic aromatic hydrocarbons reduction. *J. Phys. Chem. C* **2011**, *115* (32), 16001.
- (40) Dias, J. R. The most stable class of benzenoid hydrocarbons– new topological correlations of strain-free total resonant sextet benzenoids. *J. Chem. Info. Comp. Sci.* **2004**, *44* (4), 1210.
- (41) Grzybowski, M.; Sadowski, B.; Butenschön, H.; Gryko, D. T. Synthetic applications of oxidative aromatic coupling—from biphenols to nanographenes. *Angew. Chem. Int. Ed.* **2020**, *59* (8), 2998.
- (42) King, B. T.; Kroulik, J.; Robertson, C. R.; Rempala, P.; Hilton, C. L.; Korinek, J. D.; Gortari, L. M. Controlling the Scholl reaction. *J. Org. Chem.* **2007**, *72* (7), 2279.
- (43) Zhai, L.; Shukla, R.; Rathore, R. Oxidative C–C bond formation (Scholl reaction) with DDQ as an efficient and easily recyclable oxidant. *Org. Lett.* **2009**, *11* (15), 3474.

- (44) Tommasini, M.; Lucotti, A.; Alfè, M.; Ciajolo, A.; Zerbi, G. Fingerprints of polycyclic aromatic hydrocarbons (PAHs) in infrared absorption spectroscopy. *Spectrochim. Acta A* **2016**, *152*, 134.
- (45) Bauschlicher, C. W.; Langhoff, S. R. The calculation of accurate harmonic frequencies of large molecules: the polycyclic aromatic hydrocarbons, a case study. *Spectrochim. Acta A* **1997**, *53* (8), 1225.
- (46) Bauschlicher Jr, C. W.; Bakes, E. L. O. Infrared spectra of polycyclic aromatic hydrocarbons (PAHs). *Chem. Phys.* **2000**, *262* (2-3), 285.
- (47) Peeters, E.; Bauschlicher Jr, C. W.; Allamandola, L. J.; Tielens, A. G. G. M.; Ricca, A.; Wolfire, M. G. The PAH emission characteristics of the reflection nebula NGC 2023. *The Astrophysical Journal* **2017**, *836* (2), 198.
- (48) Bauschlicher Jr, C. W.; Ricca, A.; Boersma, C.; Allamandola, L. J. The NASA Ames PAH IR spectroscopic database: Computational version 3.00 with updated content and the introduction of multiple scaling factors. *The Astrophysical Journal Supplement Series* **2018**, *234* (2), 32.
- (49) Boersma, C.; Bregman, J.; Allamandola, L. J. Properties of polycyclic aromatic hydrocarbons in the northwest photon dominated region of NGC 7023. II. Traditional PAH analysis using k-means as a visualization tool. *The Astrophysical Journal* **2014**, *795* (2), 110.
- (50) Boersma, C.; Bregman, J. D.; Allamandola, L. J. Properties of polycyclic aromatic hydrocarbons in the northwest photon dominated region of NGC 7023. I. PAH size, charge, composition, and structure distribution. *The Astrophysical Journal* **2013**, *769* (2), 117.
- (51) Frisch, M. J.; Trucks, G. W.; Schlegel, H. B.; Scuseria, G. E.; Robb, M. A.; Cheeseman, J. R.; Scalmani, G.; Barone, V.; Mennucci, B.; Petersson, G. A. Gaussian 09 Revision D. 01, 2009. *Gaussian Inc. Wallingford CT* **2009**.
- (52) Bootsma, A. N.; Wheeler, S. E. Popular Integration Grids Can Result in Large Errors in DFT-Computed Free Energies. *ChemRxiv. Preprint* **2019**.

Experimental

Computations. Equilibrium geometries of all structures were computed at the DFT level of theory using the Gaussian 09 Rev. D.01 program,⁵¹ using the B3LYP functional and 4-31G basis set. For all computations the convergence criteria were set to tight (Opt = tight; Max. Force = $1.5 \cdot 10^{-7}$, Max. Displacement = $6.0 \cdot 10^{-7}$), and an internally defined super-fine grid size was used (SCF = tight, Int = VeryFineGrid), which is a pruned 175,974 grid for first-row atoms and a 250,974 grid for all other atoms.⁵² All stationary points found were checked to constitute true local minima, by the absence of negative frequencies.

Supplementary Figure

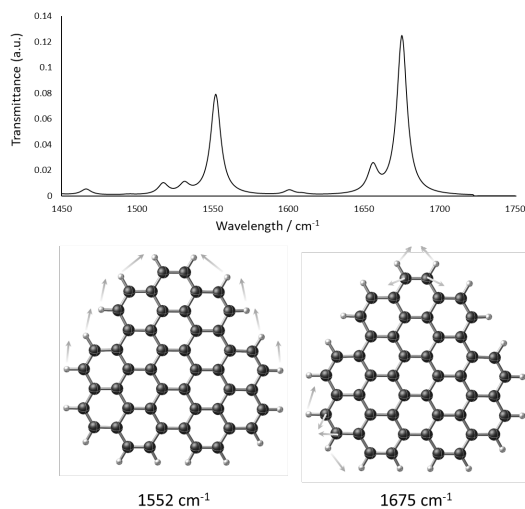


Figure S6.1 Computed anomalous vibrations observed for circum(30)triphenylene.